Journal of Structural Geology, Vol. 8, No. 6, pp. 655 to 668, 1986
Printed in Great Britain

0191-8141/86 $03.00 + 0.00
Pergamon Journals Ltd.

Calcite fabrics around folds as indicators of deformation history

DOROTHEE DIETRICH

Geologisches Institut, ETH Zentrum, CH-8092 Zürich, Switzerland

(*Received* 19 *December* 1984; *accepted in revised form* 22 *October* 1985)

Abstract—In the Morcles nappe (lowermost Helvetic nappe in western Switzerland) two phases of folding have been established. In this article the relationship between the calcite fabrics present in folded limestones and the folding history is analysed. Calcite fabrics around the first- and second-phase folds are related to the second phase of deformation. The following fabric patterns have been found. (1) The fabric geometry around a second-phase fold from the most internal part of the inverted limb of the nappe (locality Saillon) can be related to an overall simple shear deformation sequence, the sense of shear being related to the last advance of the Morcles nappe over the underlying autochthonous sedimentary cover of the Aiguilles Rouges massif. (2) In more external parts of the inverted limb (locality Petit Pré) the fabrics around a second-phase fold are interpreted as indicating a change in the deformation history from simple shear to a strain regime which can account for shortening along the first-phase cleavage by the formation of buckle folds. This change in the local strain regime could be related to a 'locking' of the frontal folds of the nappe during the last overthrust shear movements. (3) In the normal limb of the nappe the fabrics around a late second-phase kink fold (locality Neimia) are earlier than the folding event and appear to be rotated passively by the fold. (4) The fabrics around a first-phase fold (locality La Routia) are later than the folding event and overprint the fold.

INTRODUCTION

THE EXISTENCE of two phases of folding in the Morcles nappe (lowermost Helvetic nappe in western Switzerland) has been clearly shown by Badoux in his cross-section (1971) and memoir (1972). The first-phase folds are major folds related to the overall nappe structure; the second-phase folds refold the first-phase folds, the associated phase-1 cleavage and the phase-1 stretching lineation. A crystallographic preferred orientation of calcite is found in the competent, fine-grained limestones of the Morcles nappe (Schmid *et al.* 1981, Dietrich & Song 1984). The question to be discussed in this paper is how the development of the calcite fabric is related to the folding history of the nappe, and what inferences on the genesis of the individual folds can be drawn from the geometry of the calcite fabrics.

Previous investigations of calcite preferred orientation in limestones have used specimens from unfolded sectors of the Helvetic nappes of western Switzerland (Dietrich *et al.* 1981, Schmid *et al.* 1981, Dietrich & Song 1984, Dietrich & Durney in press). All the specimens showed a macroscopically predominant planar fabric defined by millimetric to submillimetric seams of clay minerals. This fabric could be correlated with the phase-1 cleavage and locally it is so strong that it obliterates the bedding. The corresponding grain shape fabric visible in thin section consists of elongate grains, which are oblique to the macroscopic cleavage (Fig. 1). The sense of obliquity between grain long axes and macroscopic cleavage is systematic and can be related to the sense of the overthrust shear movements of the nappes. The texture patterns obtained were used to infer the *c*-axis directions. The *c*-axis direction was found to be subperpendicular to the *XY* plane or flattening plane, defined by the grain shape fabric. It was deduced that the shear sense associated with the obliquity of the grain shape and crystallographic fabric is from the *c*-axis point maximum towards the normal to the macroscopic cleavage. For a detailed interpretation of the previous results see Schmid *et al.* (1981) and Dietrich & Song (1984).

It is well known that the *c*-axis fabric of calcite tectonites may be related to the kinematics of deformation. Experiments of coaxial deformation of calcite rocks to high strains at 300–600°C have consistently shown that the *c*-axes are located on a small circle at 26° to σ_1 (e.g. Turner *et al.* 1956, Rutter & Rusbridge 1977). Experiments of specifically noncoaxial deformation, under conditions where intracrystalline deformation is important (i.e. the fabric changes are produced by twinning on *e* and slip on *r*, Turner *et al.* 1956, Wenk *et al.* 1973, Casey *et al.* 1978), have likewise shown that the *c*-axis maxima produced are parallel to the axis of greatest finite shortening (Friedman & Higgs 1981).

A proposal to interpret the Helvetic fabrics on the basis of these results was put forward by Dietrich & Song (1984). The observed obliquity between the grain long axes and the macroscopic cleavage and the grain axial ratios were suggested to be a function of the strain associated with a second-phase deformational event, which overprints the macroscopically predominant phase-1 cleavage. In this paper fabric analyses around first- and second-phase folds have been undertaken in an attempt to establish the relationship of the grain shape fabric to the cleavages associated with the two folding phases, and to date the texture development relative to the folding history of the nappe.

Specimens were collected around five first-phase folds and around three second-phase folds of the Morcles nappe. The positions of the folds investigated in a profile

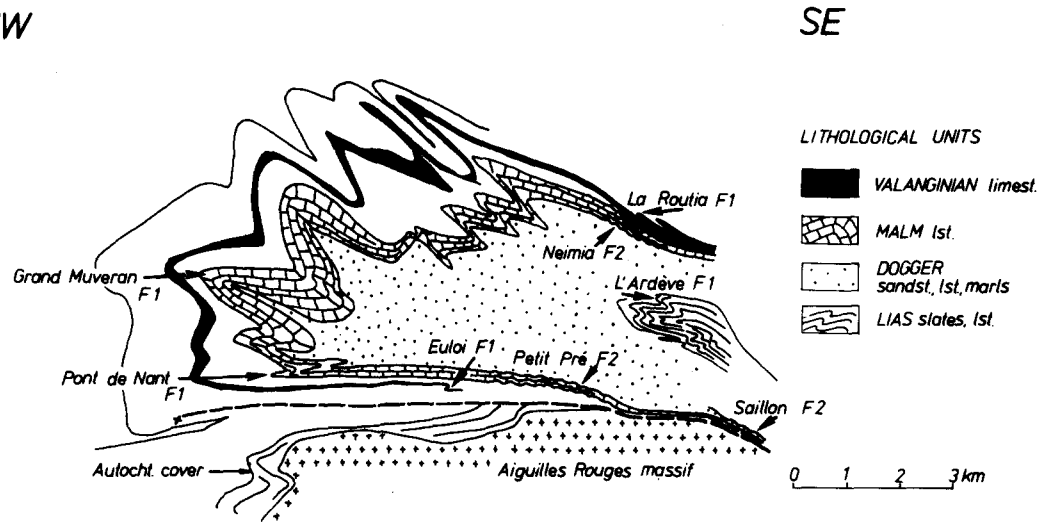

Fig. 2. A profile (down-plunge projection) through the Morcles nappe. The F_1 and F_2 investigated folds are indicated.

section of the nappe are indicated in Fig. 2. The locality coordinates and lithological and orientation data of the individual specimens are listed in Table 1.

METHOD OF MEASUREMENT AND GRAPHICAL REPRESENTATION OF TEXTURE DATA

The preferred orientation of the specimens was determined by X-ray techniques, using the texture goniometer at the Geologisches Institut, ETH Zürich (combined reflection- and transmission-scan method, CoKα-radiation, counting time 50 s for each 5° step in azimuth and tilt and 100 s on two background positions after every increment tilt, see Casey *et al.* 1978, Schmid *et al.* 1971 and Siddans 1976).

Instead of measuring directly the *c*-axis preferred orientation, the orientation of the calcite *a*-planes was measured. This was done because the intensity of the *a* or [11$\bar{2}$0] diffraction peak is about four times higher than the intensity of the *c* or [0001] peak, and therefore easier to measure. Direct measurements of the *c*-axis preferred orientation by texture goniometry and U-stage methods have shown a single maximum pattern, which coincides with the *a*-minimum in the pole figures obtained (Schmid *et al.* 1981, Dietrich & Song 1984). The *c*-maxima (as the *a*-minima) are fairly broad and represent, according to experimental work (e.g. Turner *et al.* 1956), a preferred

Table 1. Lithological and orientation data of the specimens studied

Fold	Phase	Age and formation name of folded strata	Coordinates of fold hinges	Specimen	Specimen orientation (strike/dip of bedding for F_1 folds, of F_1 cleavage for F_2 folds)	Lithology	Grain long axis (average) mm
La Routia	F_1	Lower Cretaceous Valanginian limest.	584.25/117.95	D 673	28/60 SE	limestone with rare quartz clasts	0.2 bigger grains 0.02 matrix
				D 674	34/62 SE (inverted limb)		
				D 675	37/61 NW		
L'Ardève	F_1	Lower Jurassic Middle Liassic	581.25/116.50	D 679	no calcite preferred orientation	sandy limestone with clay seams thicker than 1 μ	0.15 bigger grains 0.015 matrix
				D 680			
				D 681			
Grand Muveran	F_1	Upper Jurassic Upper Malm	577.87/124.40	D 575.0	no calcite preferred orientation	biomicrite	0.2 bigger grains 0.002 matrix
				D 576.0			
				D 577.0			
				D 580.0			
Pont de Nant	F_1	Upper Jurassic Upper Malm	574.95/121.15	D 646	no calcite preferred orientation	biomicrite	0.1 bigger grains 0.002 matrix
				D 647			
				D 648			
Euloi	F_1	Lower Cretaceous Valanginian limest.	574.65/116.75	D 676	no calcite preferred orientation	sandy limestone	0.1 bigger grains 0.005 matrix
				D 677			
				D678			
Saillon	F_2	Middle Jurassic Lower Bajocian	579.80/113.15	D 641	63/84 SE	limestone with rare quartz clasts	0.05 bigger grains 0.01 matrix
				D 642	91/10 S		
				D 643	43/17 NW		
Petit Pré	F_2	Upper Jurassic Upper Malm	576.77/115.90	D 566	258/65 N (inverted limb)	limestone with pellets	0.15 bigger grains 0.015 matrix
				D 567	23/70 SE		
				D 568	275/61 N		
				D 698	66/64 NW (inverted limb)		
				D 699	310/48 NE		
Neimia	F_2	Upper Jurassic Upper Malm	583.85/118.05	D 670	43/82 SE	limestone with pellets	0.04 bigger grains 0.02 matrix
				D 671	325/04 NE (inverted limb)		
				D 672	38/39 SE (inverted limb)		

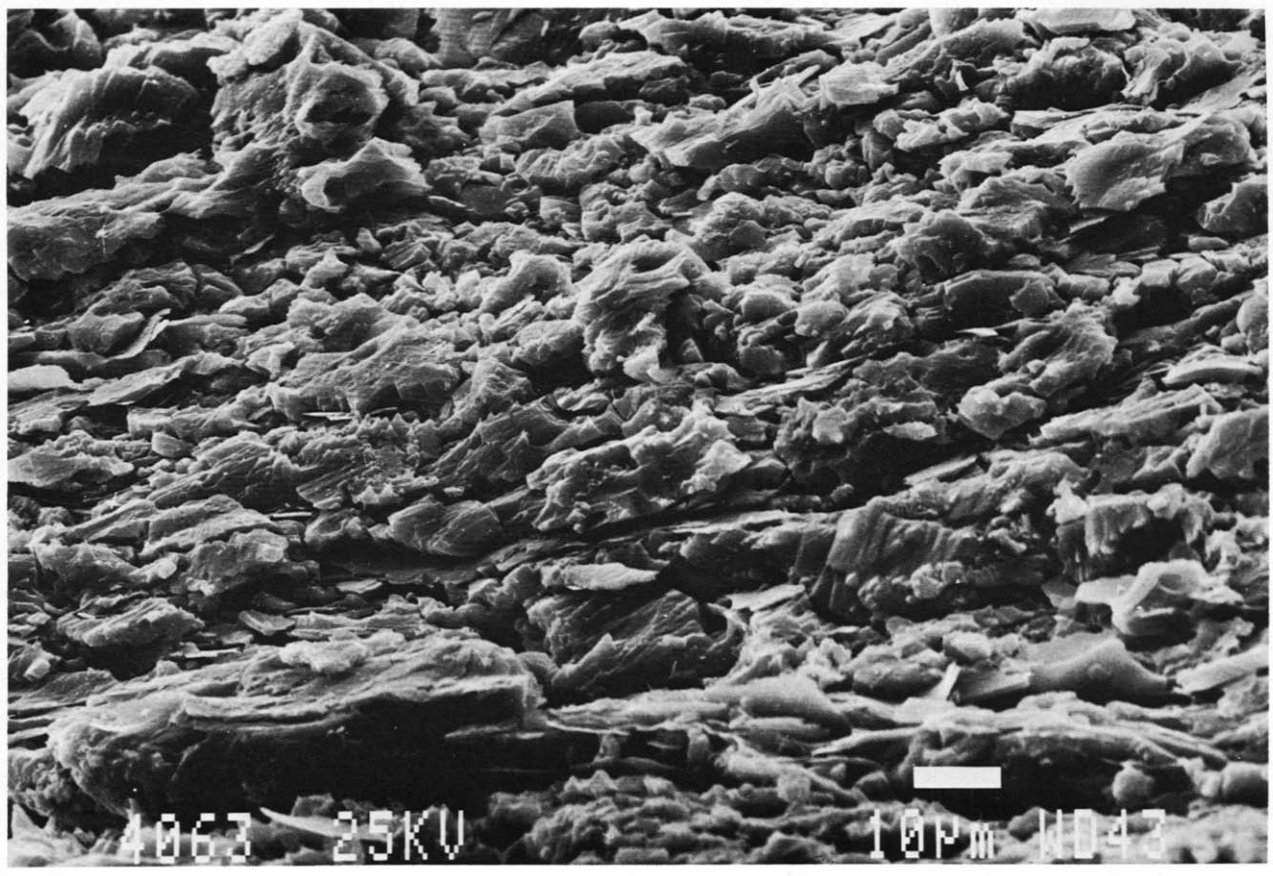

Fig. 1. Scanning EM-micrograph of a typical Helvetic limestone with a crystallographic preferred orientation. The specimen shows the macroscopically predominant planar cleavage, which is horizontal in the micrograph. The grain-shape fabric is oblique relative to the macroscopic cleavage. The shear sense relative to the micrograph is dextral. Lower Cretaceous Valanginian limestone at Ardon, normal limb of the Morcles nappe. Scale bar is 10 μm.

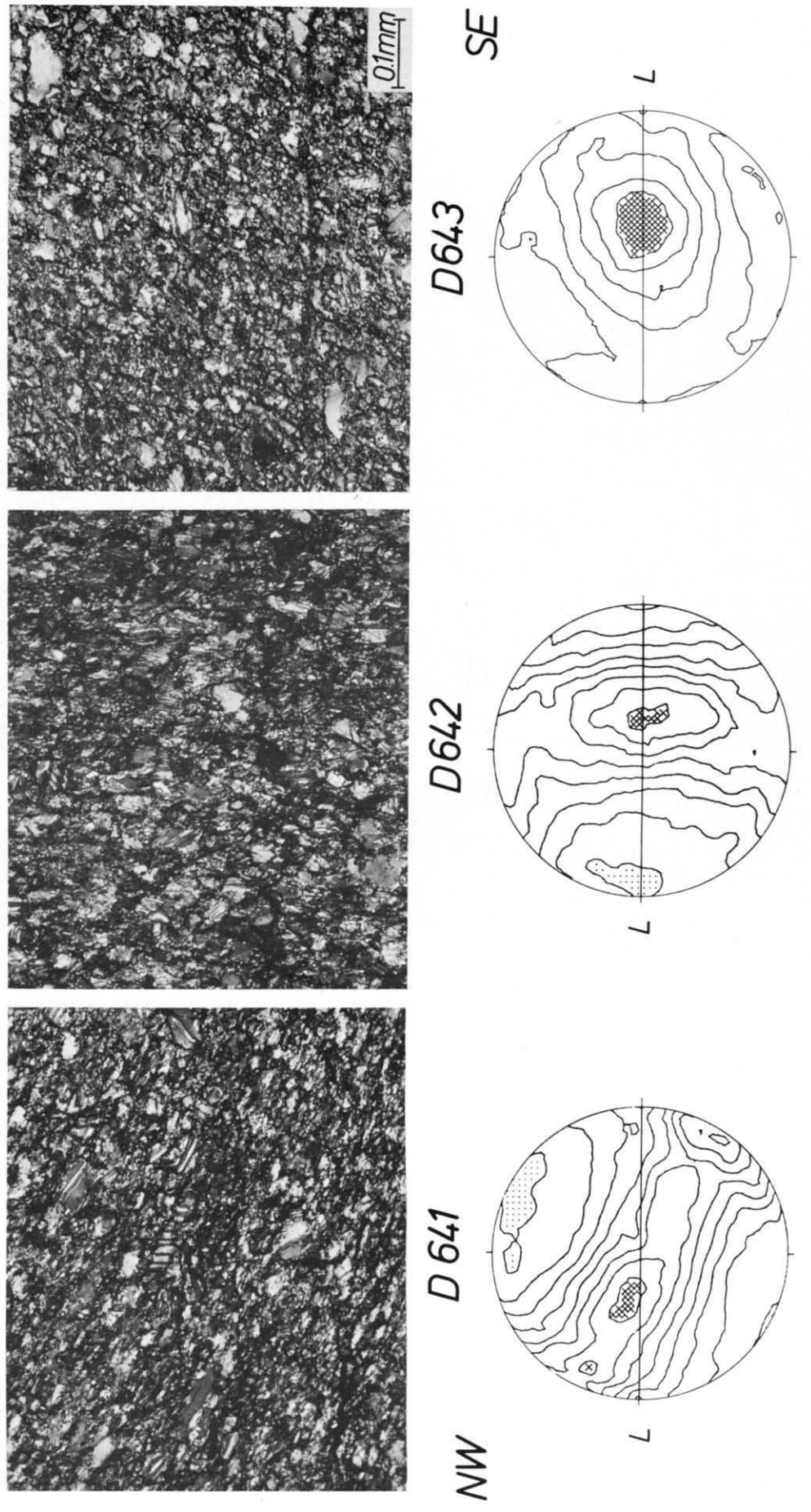

Fig. 4. F_2 fold at Saillon, comparison of microstructures and textures. The F_1 cleavage is horizontal in the micrographs and indicated with a horizontal line in the pole figures. The scale is identical in all the micrographs. The orientation of the micrographs and pole figures is perpendicular to the F_1 cleavage and parallel to the stretching lineation. The pole figures are upper-hemisphere equal-area projections. L, stretching lineation. The intensity maxima are 1.9 for 641 and 642, 1.8 for 643. The difference in the intensity maxima of the rotated and unrotated pole figures is an artefact of the contour smoothing process.

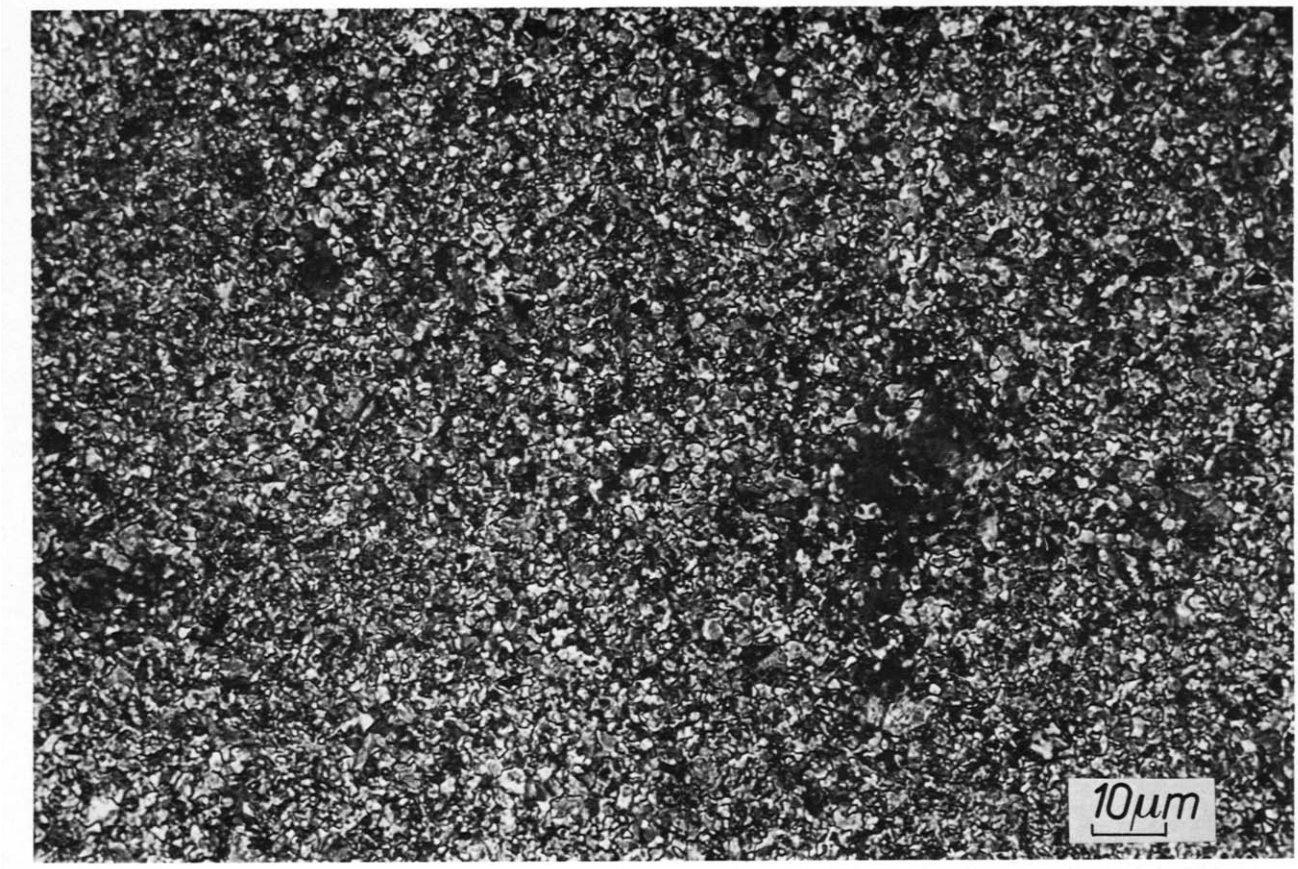

Fig. 11. Micrograph of a typical Helvetic limestone without a crystallographic preferred orientation. No shape preferred orientation of the grains is visible. The grain size is extremely small if compared with the grain sizes of specimens shown in Figs. 1, 4 and 13. Hinge area of the Grand Muveran F_1 fold, specimen D 576.0.

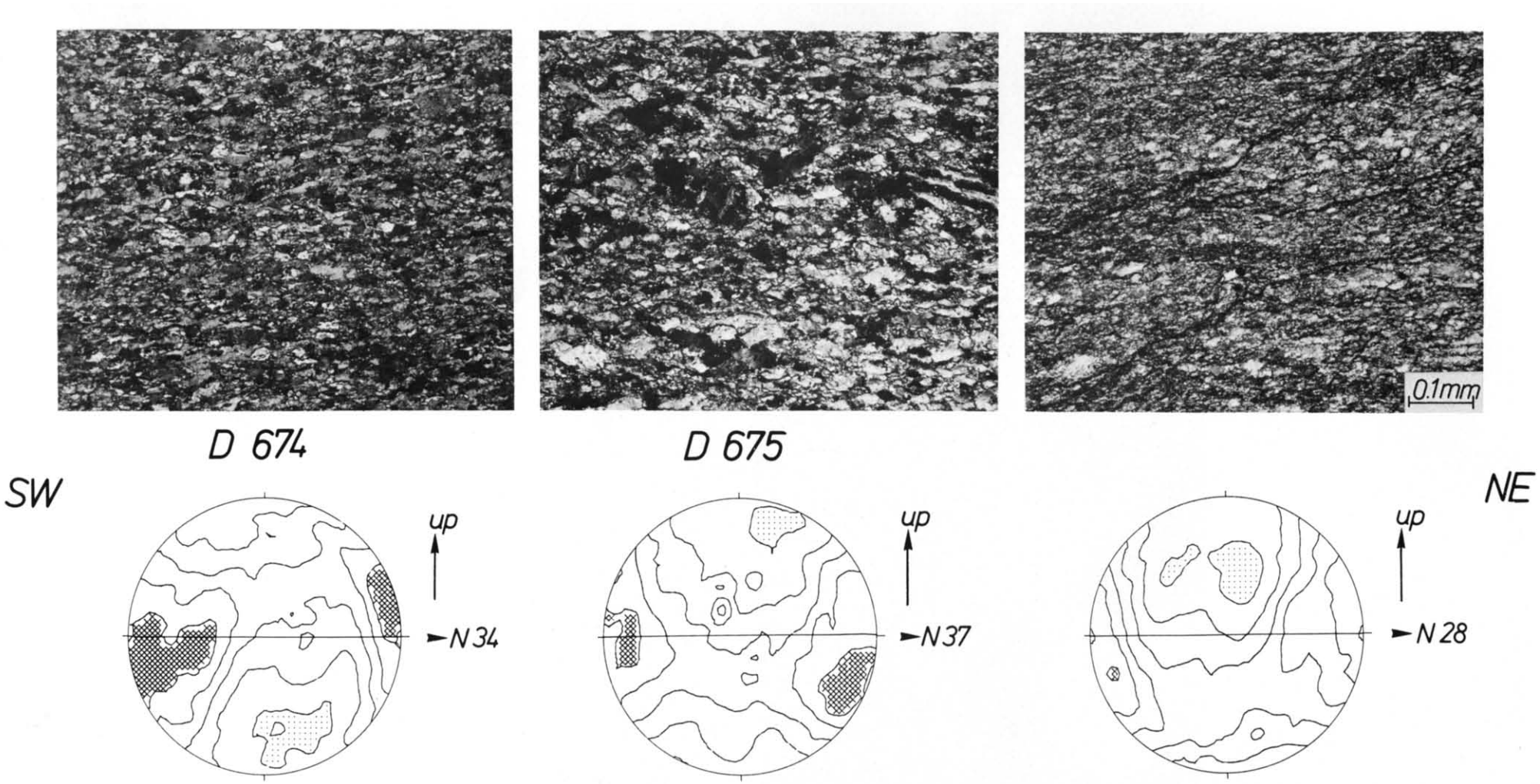

Fig. 13. F_1 fold at La Routia, comparison of microstructures and textures. Bedding is horizontal in the micrographs and indicated with a horizontal line in the pole figures. The scale is identical in all the micrographs. The orientation of the micrographs and pole figures is perpendicular to the bedding and parallel to the fold axis. The pole figures are upper-hemisphere equal-area projections. The intensity maximum is 1.6 for all three pole figures.

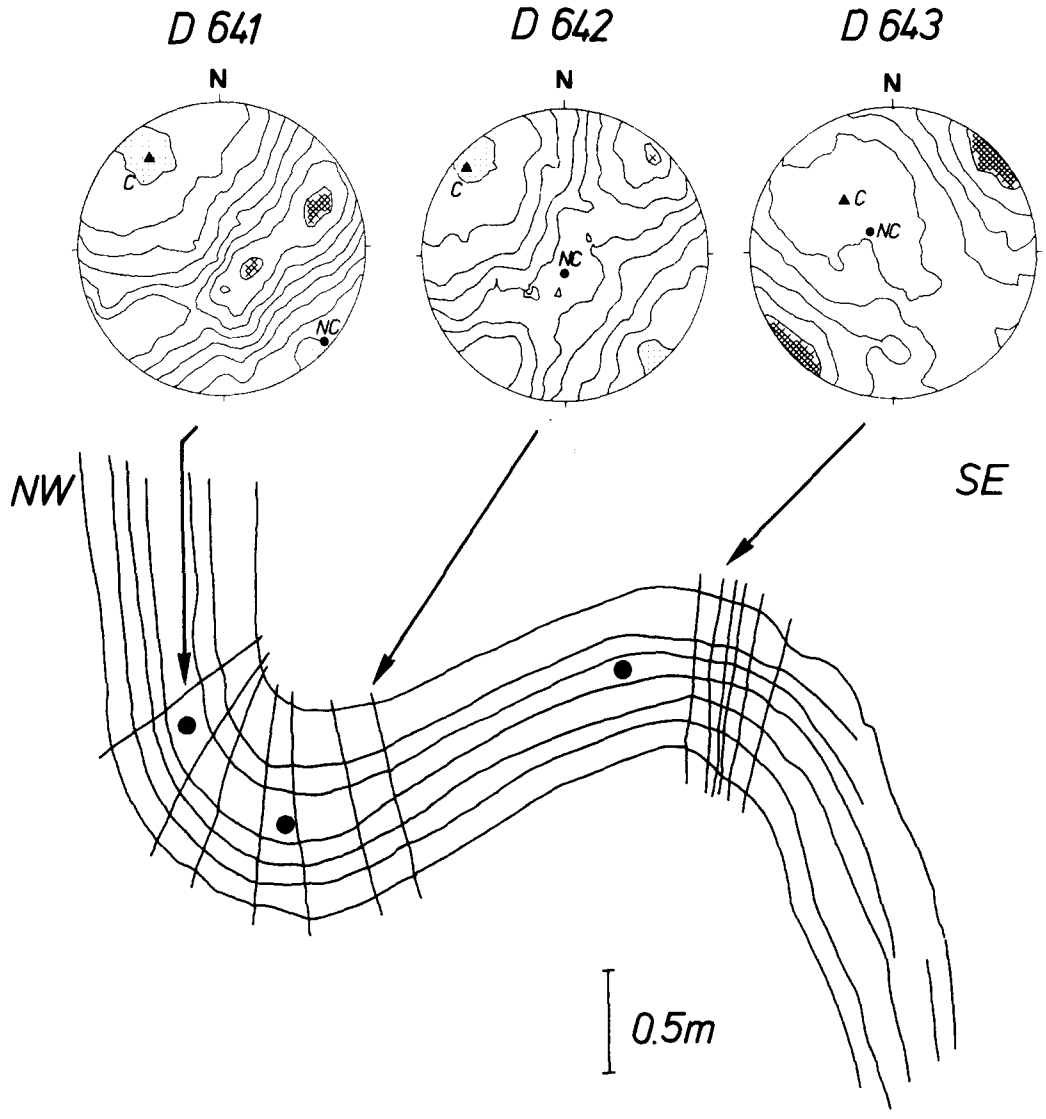

Fig. 3. F_2 fold at Saillon, inverted limb of the Morcles nappe, Middle Jurassic limestones. A well-developed F_1 cleavage is folded by an F_2 fold. The pole figures, upper-hemisphere equal-area projections, are in geographical coordinates and show the preferred orientation of calcite *a*-planes. The stipple pattern indicates the region of the *a*-minimum or *c*-maximum. c, *c*-axis maximum; NC, normal to the phase-1 cleavage. The cross-hatched pattern indicates the region of the *a*-maximum. The intensity maxima are 1.9 for 641 and 642, 1.7 for 643.

orientation of the compression directions (*c*-axis location on a 26° small circle around σ_1).

The preferred orientation of the *a*-planes is represented in this article in upper-hemisphere equal-area projections. A rotation of the pole figures of 180° around the projection centre converts an upper-hemisphere projection to a lower-hemisphere projection. For all the specimens measured a pole figure in geographical coordinates is given, that is north on the pole figure corresponds with geographical north. For several specimens also an equal-area projection of the *a*-poles with respect to the specimen coordinates is given. In these cases the pole figures are oriented perpendicular to the phase-1 cleavage and parallel to the phase-1 stretching lineation, so that the phase-1 cleavage corresponds with the equator in the pole figures. The contours of the pole figures represent multiples of a uniform distribution; the contour intervals are 0.2, and the maximum intensity values are indicated in the figure captions.

FABRICS AROUND SECOND-PHASE FOLDS

The second-phase fold at Saillon

Figure 3 shows a second-phase fold in the highly deformed Middle Jurassic limestones at Saillon from the inverted limb of the Morcles nappe. The macroscopically predominant planar fabric, which is folded, corresponds to the phase-1 cleavage. Bedding is subparallel to the cleavage and cannot be distinguished from it. A stretching lineation is seen on the cleavage plane and is deformed by the fold. A second-phase cleavage is developed which converges from the outer arc towards the inner arc of the fold. The dip isogons are also convergent and the fold is a class 1C fold (Ramsay 1967). The traces of the fold cleavage are not mirror symmetric on either side of the fold axial plane. It will be shown below that this geometry probably relates to a component of sinistral shear during the folding process.

The three pole figures obtained from this fold are also shown in Fig. 3. They are in geographical coordinates. There exists an evident preferred orientation of the calcite *a*-planes, but the D 641 and the D 642 pole figures show an orientation pattern different from D 643. In D 641 and D 642 there exists a great-circle distribution of the *a*-poles with a tendency for the development of a maximum in the great circles. D 643 shows a stronger *a*-maximum which obliterates the great-circle pattern. The inferred *c*-maxima (or *a*-minima) have azimuth directions towards SE in all the three pole figures, whereas the dips are subhorizontal for D 641 and D 642, and 50° for D 643. The shear direction from the *c*-maximum to the normal to the cleavage is towards the NW for D 641 and D 642, and towards the SE for D 643. The angles between the *c*-axis maxima and the normals to the cleavage are 29° for D 641, 92° for D 642 and 23° for D 643.

The existence of different orientation patterns around the fold indicates that the calcite fabrics have not overprinted the fold uniformly and were therefore not acquired after the folding event. The fact that the angles between the *c*-maxima and the normals to the cleavage vary in the three pole figures also suggests that the fabrics were not acquired before the folding event and later passively rotated during folding. The fabric appears to be genetically related to the second-phase fold.

A different representation of the same data, shown in Fig. 4, allows a discussion of the relationship of the fabric to the second-phase folding event. The micrographs and the pole figures in Fig. 4 have the same orientation: they are both from sections perpendicular to the phase-1 cleavage and parallel to the stretching lineation. The phase-1 cleavage is horizontal in the micrographs and is indicated in the pole figures with a line which corresponds with the equator. The stretching lineation, updip in upper hemisphere projection, is labelled '*L*' on the pole figures.

The phase-1 cleavage can be recognized in all the three micrographs of Fig. 4 by a horizontal alignment of ore minerals relative to the micrographs. The grain shape fabric of D 641 and D 642 is seen as a well-defined elongation of the individual grains, and is clearly oblique to the phase-1 cleavage. D 643 shows a weakly developed grain shape fabric. Only the larger intraclasts are elongate parallel to the *a*-girdle in the corresponding pole figure. The elongate grains define a fabric plane dipping at about 20° to the left of the micrograph. The matrix grains do not show a clear shape preferred orientation. A few μm thick seams of clay minerals dip at 65° towards the left. Under the microscope these seams appear to be crosscut by the larger intraclasts, that is the grain shape fabric is younger than the clay seams. The broad *a*-girdle in the corresponding pole figure is subparallel to the long axes of the larger intraclasts in the micrograph.

The following observations can be made.

(1) For all the specimens there is a noncoincidence between grain shape fabric and the macroscopically predominant phase-1 cleavage, in accordance with the observations of Schmid *et al.* (1981) and Dietrich & Song (1984).

(2) Grain shape fabric and crystallographic fabric are parallel. The obliquity of the grain shape fabric relative to the phase-1 cleavage corresponds with the obliquity of the calcite *a*-girdles relative to the phase-1 cleavage.

(3) In D 641 and D 642 both grain shape and crystallographic fabric are parallel to the phase-2 cleavage which is related to the fold. This appears evident from the rotated pole figures in Fig. 3. The *c*-axis maxima (or *a*-minima) are therefore parallel to the normals to the phase-2 cleavage planes. In other words: the compression directions which can be inferred from the crystallographic fabric correspond with the compression directions which can be inferred from the fold-related cleavage fan.

(4) If we extrapolate the cleavage fan indicated in Fig. 3 to the D 643 locality, the steeply dipping clay seams at that locality would be parallel to the fold-related cleavage fan. In fact, in all three hand specimens analysed from this locality a macroscopically visible phase-2 cleavage coincides with the clay seams. The grain shape and the crystallographic fabric of D 643 are less inclined than the clay seams and cannot simply represent the fold-related cleavage in that particular region of the anticline. This appears evident from the orientation of the crystallographic fabric of D 643 in Fig. 3.

Casey & Huggenberger (1985) have shown by numerical modelling that, for the development of the folds in the Morcles nappe, simple shear bulk deformation can be assumed. Small initial perturbations, if deformed under heterogeneous simple shear, develop into folds with geometric characteristics comparable to the folds observed in nature. Ramsay *et al.* (1983, fig. 4) give a graphical representation of this idea. If this modelling procedure is accepted, the following geometric model for the development of the Saillon fold can be envisaged (Fig. 5). The macroscopic cleavage planes which are shown folded in Fig. 3 are well-marked surfaces along which shearing deformation during the production of the second-phase folds was relatively easy. In Saillon,

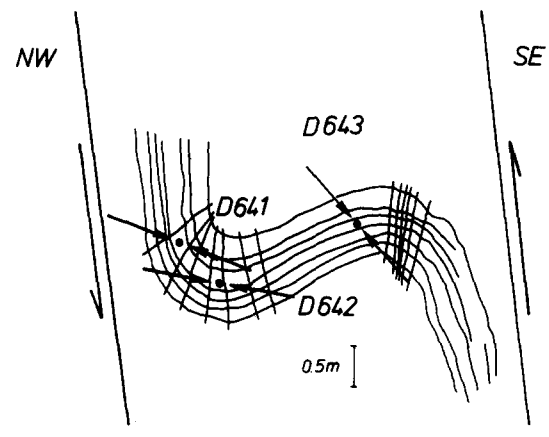

Fig. 5. A model for the development of the F_2 fold at Saillon. The compression directions inferred from the textures are indicated. The fold is represented in a profile section.

the average dip of these cleavage planes is subparallel to the main thrust contact at the base of the nappe (Fig. 2). In Fig. 5 the shear planes associated with the formation of the fold being discussed appear to be subparallel to the main thrust contact.

In most shear zones the finite strain axes and the infinitesimal strain and stress axes are not parallel. The incremental strain axes and principal stress directions are oriented at 45° to the shear zone boundary planes, whereas, with progressive shearing, the angle between the short axis of the finite strain ellipsoid and the shear boundary planes increases (Ramsay 1980). The compression directions (or *c*-axis directions) derived from the pole figures of Fig. 3 are indicated in Fig. 5. The angles between the D 641 and the D 642 compression directions and the shear zone boundary planes are greater than 45°, indicating that the two compression directions represent the finite strain axes rather than infinitesimal strain or stress axes in the shear zone. The angle between the D 643 compression direction and the shear zone boundary planes is close to 45°. At this point it must be recalled that the shear direction from the *c*-maximum towards the normal to the phase-1 cleavage of the D 643 pole figures is from NW to SE, that is opposite to the regional shear sense deduced, for example, from Fig. 2. The fold limb on which D 643 is situated appears to have been rotated by the shear zone shown in Fig. 5. The fold-related cleavage fan, represented by the clay seams in D 643, is therefore assumed to have been rotated with the limb. The compression directions associated with the cleavage fan rotated in the extensional quadrant of the shear zone. A new fabric, the observed grain shape and crystallographic fabric was established, which overprinted the cleavage fan. In fact, the shear direction from the D 643 *c*-axis maximum towards the normals to the planes of the cleavage fan is from SE towards NW. The D 643 fabric could therefore be interpreted as representing a late adjustment of the fold limb to progressive rotational deformation.

In conclusion, it appears possible to explain the fabrics of the Saillon fold using the geometric features of simple shear deformation. This simple shear deformation corresponds to the last overthrust movement of the Morcles nappe and the overlying Helvetic nappes over the autochthonous sedimentary cover of the Aiguilles Rouges massif. The phase-1 cleavage locally became folded, and the calcite fabrics around the Saillon fold together with the fabrics in the unfolded parts of the nappe in the root zone, can be related to this second-phase deformation.

The second-phase fold at Petit Pré

Second phase folds which affect the phase-1 cleavage and stretching lineation are common in the inverted limb of the Morcles nappe around the alp Petit Pré. As seen at Saillon the bedding is at a very low angle to the phase-1 cleavage and macroscopically cannot easily be distinguished from it. These second-phase folds are usually fairly open folds with a metric wavelength. Figure 6 shows such a fold in the Upper Jurassic limestones. It is a convergent isogon fold (class 1C, Ramsay 1967), with an axial plane at a high angle to the regional dip of the phase-1 cleavage. Its shape appears to be modified by the superposition of a plane strain or flattening strain component with a shortening direction subperpendicular to the axial plane. No axial-planar cleavage is developed. The sense of the regional overthrust shear is dextral relative to the view direction in Fig. 6.

The microstructure of the specimens studied consists of a very fine grained almost pure calcite matrix (average grain size around 15 μm), in which a predominant shape preferred orientation is absent. However there exists an elongation of the individual grains.

The pole figures from different parts of this fold are shown in geographical coordinates. The poles to the *a*-planes generally show a great-circle distribution, with an *a*-maximum within the great circle. In one of the pole figures from the hinge of the fold, D 567, the great circle is obliterated by a strongly developed *a*-maximum. The *a*-great circles are subparallel to the flattening plane defined by the elongated matrix grains. In all the pole figures a clearly defined *a*-minimum is seen and from this pattern it is possible to infer the mean *c*-axis direction. The *c*-axis direction varies in orientation around the fold and it does not generally coincide with the normal to the phase-1 cleavage. The crystallographic fabric is therefore neither overprinting the fold uniformly, nor is it simply related to the phase-1 cleavage. The fabric appears to be genetically linked to the formation of the second-phase fold. The shear direction deduced from the relations between the *c*-maximum and the normal to the cleavage is opposite in the two limbs of the syncline. The direction from the *c*-maximum towards the normal to the cleavage is from W to E or from NW to SE for D 568 and D 699, and from SE to NW for D 566, D 698 and D 567.

There are distinct geometric differences between the previously discussed fold at Saillon and the Petit Pré fold. Figure 7 is a profile section through the Petit Pré fold. The folded phase-1 cleavage plane and the *c*-axis directions inferred from the pole figures of Fig. 6 show dip values referred to the profile section. The average dip of the phase-1 cleavage at Petit Pré determined from the profile of Fig. 2 is 25° towards the SE. The fabrics around this fold, and the high angle of the axial plane relative to the regional dip of the phase-1 cleavage cannot be explained within an overall deformation scheme of simple shear.

The orientation pattern of originally rectilinear structures which are deformed by folding can give indications on the particular deformational regime under which the fold developed. Ramsay (1967) has discussed the geometry of linear structures deformed by folds with various deformation histories. If a fold forms via layer displacement by heterogeneous simple shear the deformed lineations should lie on a plane locus and plot on a great circle in a projection. In contrast, the lineation geometry in a flexural-slip fold is controlled by a con-

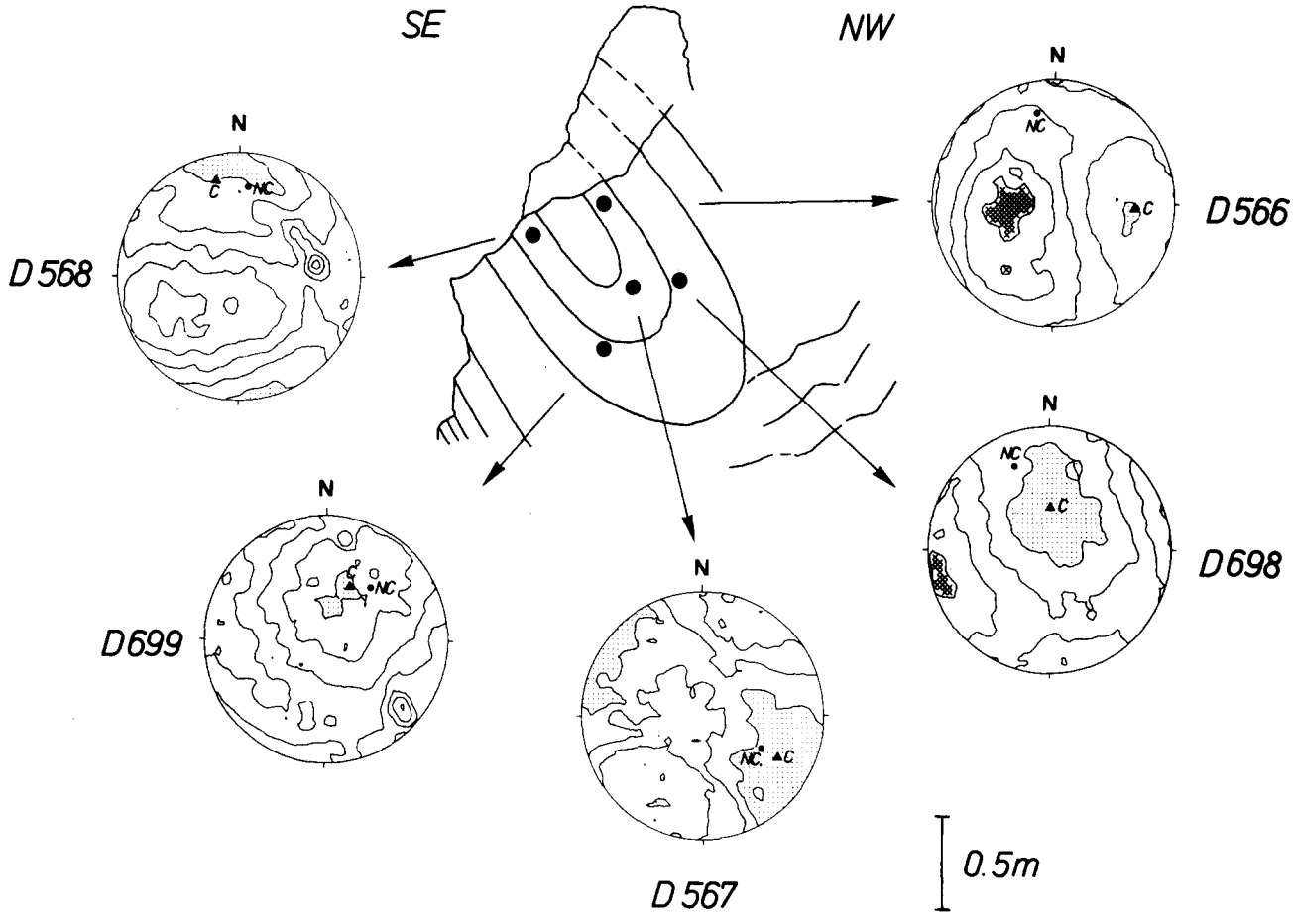

Fig. 6. F_2 fold at Petit Pré, inverted limb of the Morcles nappe, Upper Jurassic limestones. A well-developed F_1 cleavage is folded by an F_2 fold. The pole figures, upper-hemisphere equal-area projections, are in geographical coordinates. c, *c*-axis maximum; NC, normal to the phase 1 cleavage. The intensity maxima are 1.6 for 566, 1.4 for 567, 1.7 for 568, 1.5 for 698, 1.8 for 699.

stancy of angle between the deformed linear structure and the fold axis at all points on the folded surface, and the lineation locus plots as a small circle. Figure 8 shows an equal-area projection of the deformed phase-1 stretching lineation measured around the Petit Pré fold.

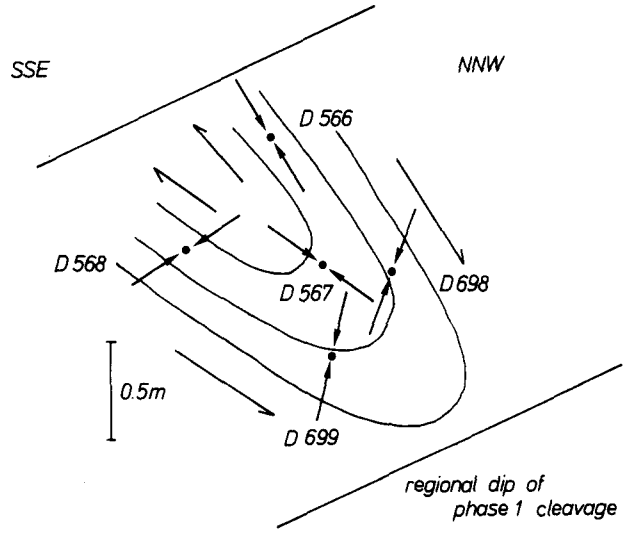

Fig. 7. A model for the development of the F_2 fold at Petit Pré. The compression directions inferred from the textures are indicated. The fold is represented in a profile section.

The lineation pattern obtained is complex but can be compared most closely with that of a flexural-slip fold modified by the superposition of a plane strain or flattening strain component. Those lineations in the eastern quadrant of the projection shown in Fig. 8, which do not lie on the lineation locus for flexural-slip folding, are located on the two fold limbs. On the fold limbs the angle between the lineations and the fold axis is greater than predicted for fold formation by flexural slip. In contrast, the angle between the group of lineations in the centre of the plot and the fold axis is smaller than predicted for flexural-slip folding. The superposition of a plane strain component with maximum shortening direction perpendicular to the axial surface of a flexural-slip fold would tend to reduce the angle between lineation and fold axis in the hinge zone, whereas it would tend to increase the angle between lineation and fold axis in the two fold limbs. This interpretation also accords with the opposite shear directions on the two fold limbs inferred from the textures in Fig. 6. If we make the reasonable assumption that the *Y*-axis of the superimposed plane strain component coincides with the fold axis, and that the *X*-axis lies in the fold axial surface, it is possible to determine the principal strain ratio λ_3/λ_1 of the plane strain component (Ramsay 1967, equation 8-4). The profile shown in Fig. 7 has been constructed according to the calculated value of the plane strain component.

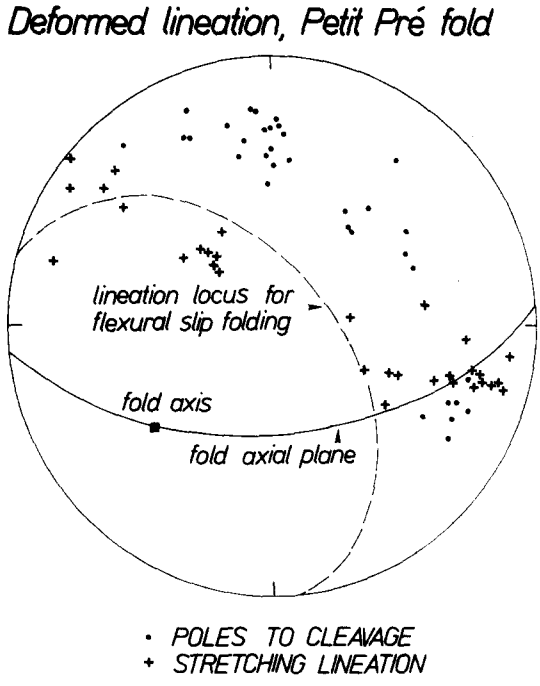

Fig. 8. Upper-hemisphere equal-area projection of structures in the Petit Pré fold.

It has been previously suggested, that the second-phase deformation in the Morcles nappe is associated with a last movement of the nappe towards the NW (Dietrich & Durney, in press, and discussion of the Saillon fold). Second-phase deformational features, however, have not been identified in the frontal or NW part of the nappe, whereas they are common in the root zone or SE part of the nappe. It is concluded that whilst the SE part of the nappe was redeformed by a last overthrust shear movement, the frontal folds did not amplify or modify their shape and were effectively 'locked'. Consequently the second-phase deformational regime changes from simple shear in the root zone towards another type of strain regime in the core of the nappe, which can account for the formation of buckle folds. This conclusion is in agreement with the different texture patterns found in the Saillon and Petit Pré folds.

The second-phase fold at Neimia

The fold investigated is a second-phase minor structure from the normal limb of the Morcles nappe and is located in a cliff of Upper Jurassic limestones above Neimia (Fig. 9). It is a class 1B fold, and its overall aspect is that of a kink fold. This fold was developed in an initially planar, pre-existing phase-1 cleavage, but no stretching lineation, such as was identified at Petit Pré, accompanies the first cleavage. No obvious fold-related cleavage fan is developed. The shear direction, as inferred from the overthrust sense of the nappe, is sinistral relative to the geometry shown in Fig. 9.

The three pole figures in Fig. 9 are in geographical coordinates and the poles to the a-planes show great-circle patterns. The orientation of the a-minima or c-maxima varies around the fold, but the angle between the c-axis maxima and the normals to the cleavage is

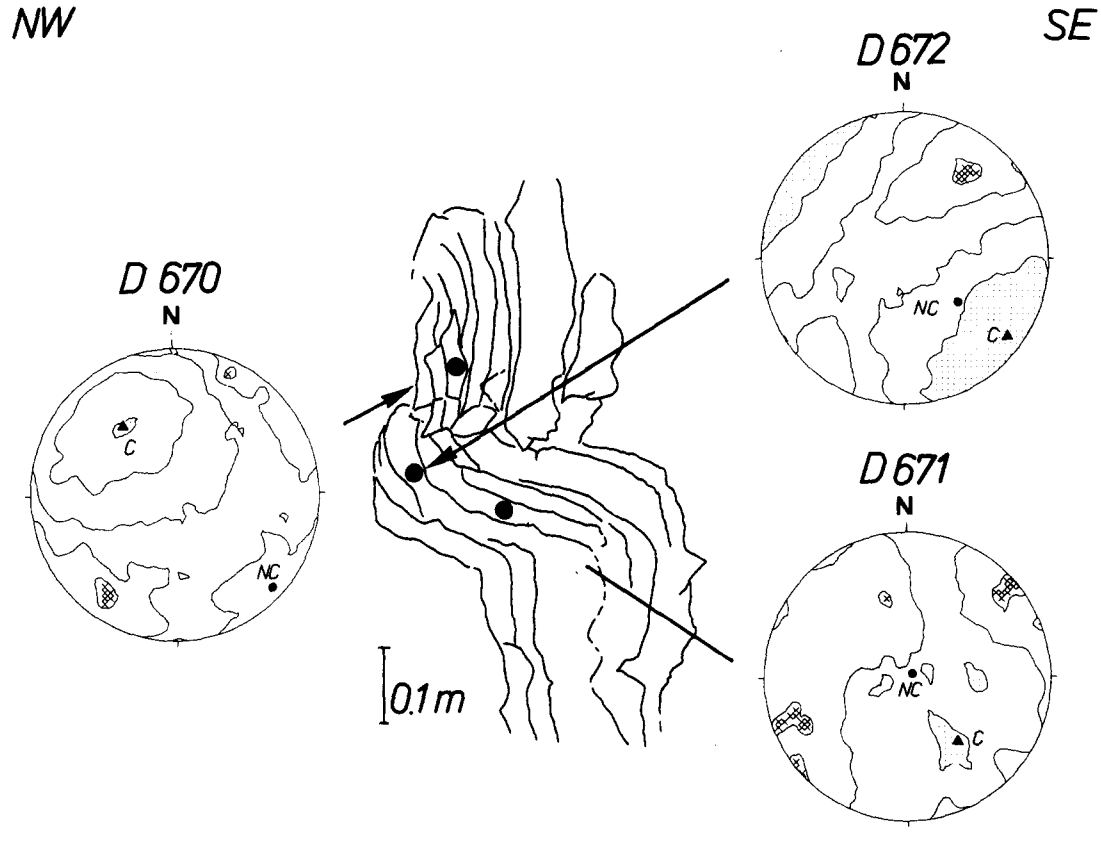

Fig. 9. F_2 fold at Neimia, normal limb of the Morcles nappe, Upper Jurassic limestones. A well-developed F_1 cleavage is folded by an F_2 fold. The pole figures, upper hemisphere equal area projections, are in geographical coordinates. c, c-axis maximum; NC, normal to the phase 1 cleavage. The intensity maxima are 1.5 for 670, 1.2 for 671, 1.5 for 672.

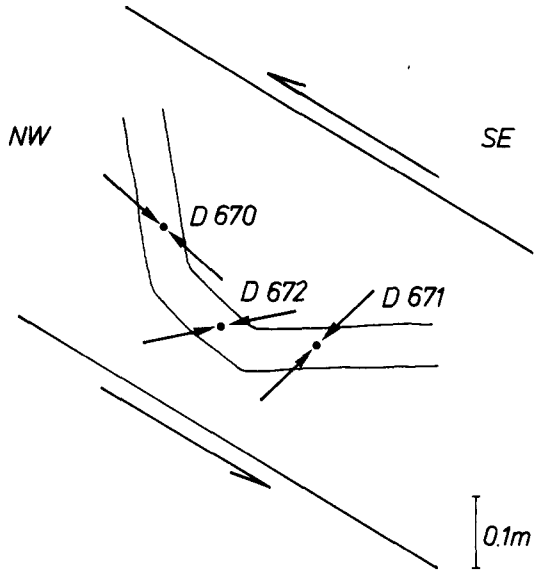

Fig. 10. A model for the development of the F_2 fold at Neimia. The compression directions inferred from the textures are indicated. The fold is represented in a profile section.

approximately constant in the fold profile (Fig. 10). It is deduced from this constancy of angle that this fold acquired its pattern of calcite preferred orientation before the formation of the fold, and that the fabric was rotated passively during the folding event. The fabric is clearly oblique to the folded phase-1 cleavage. The shear zone boundary planes indicated in Fig. 10 were constructed parallel to the regional dip of the phase 1 cleavage above Neimia. The calcite preferred orientation overprints the phase-1 cleavage and is possibly related to shear movements subparallel to the strongly developed first cleavage. The calcite fabric is therefore related to an early stage during a second-phase deformational event.

FABRICS AROUND FIRST-PHASE FOLDS

The large-scale folds of the Morcles nappe which appear in the profile of Fig. 2 are referred to as phase-1 folds (Badoux 1971, 1972, Durney 1972). The largest and most strongly developed first-phase folds occur fairly external to or north of the Helvetic root zone located in the Rhône valley (right side of Fig. 2).

The calcite preferred orientation in the Helvetic nappes of western Switzerland weakens and disappears north of the high finite strain region along the Helvetic root zone (Dietrich & Song 1984). The textures around five first-phase folds have been analysed (Fig. 2), but in only one, the fold at La Routia, was a calcite preferred orientation found. The La Routia fold lies closer to the root zone than the other four folds investigated. In the other four folds random orientation patterns were obtained. In the rocks showing no crystallographic fabric, microstructures consist of a mosaic of extremely small grains, which are an order of magnitude smaller than the grains in the specimens with a well-developed crystallographic fabric discussed previously. Figure 11 shows an example of these microstructures. The specimen is from Upper Jurassic limestone and was taken from the hinge area of the Grand Muveran fold (Fig. 2). The grains in the micrograph are equidimensional and untwinned, and have a diameter of about 2 μm.

The first-phase fold at La Routia

The La Routia first-phase fold is shown in Fig. 12. It is a class 1C fold showing convergent dip isogons. The phase-1 cleavage associated with this fold is strongly developed, but no associated stretching lineation was detected. The fold axis is subhorizontal and its position is indicated in Fig. 15.

Specimens were collected from the Lower Cretaceous Valanginian limestones. The three pole figures of Fig. 12 are in geographical coordinates and show similar preferred orientation patterns. The poles to the *a*-planes are located on great circles of a comparable position in all three pole figures. The *a*-maxima contained in the great circles are parallel to the fold axis. Figure 13 shows a comparison of microstructures and *a*-pole figures, both in the same orientation. Bedding is horizontal in the three micrographs and is indicated with a horizontal line in the corresponding pole figures. D 673 and D 674 are perpendicular to the fold-related phase-1 cleavage and subparallel to the fold axis. D 675 is parallel to the phase-1 cleavage and to the fold axis. In the micrographs of D 673 and D 674, the phase-1 cleavage is marked by clay seams which dip at a low angle towards the SW. All three micrographs show a grain shape fabric defined by an elongation of the individual grains. The average grain long axis is oblique to the bedding and the phase-1 cleavage. The grain shape fabric and the *a*-great circles are parallel.

Figure 14 is a profile section through the fold. The *c*-axis maxima inferred for the two fold limbs, D 673 and D 674, are subhorizontal and parallel, whereas the *c*-axis maximum for the fold hinge, D 675, is slightly steeper. The fabric appears not to be related to the fold itself, but overprints it. The preferred orientation patterns are markedly asymmetric to the fold and seem to be best explained as fabrics developed during the second phase of deformation. The steeper *c*-axis direction at the hinge zone, D 675, might be explained as the result of a slight late rolling of the hinge line, in accordance with the shear sense indicated in Fig. 14.

CONCLUSIONS

The fabric defined by the crystallographic preferred orientation and the grain shape in the limestones of the Morcles nappe clearly overprints the first-phase deformational structures. This has been shown by the texture analysis of the first-phase fold at La Routia, as well as by the generally observed obliquity between the inferred *c*-axis directions and the phase-1 cleavage. The fabric is therefore related to the second phase of deformation.

The *c*-axis directions around two second-phase folds

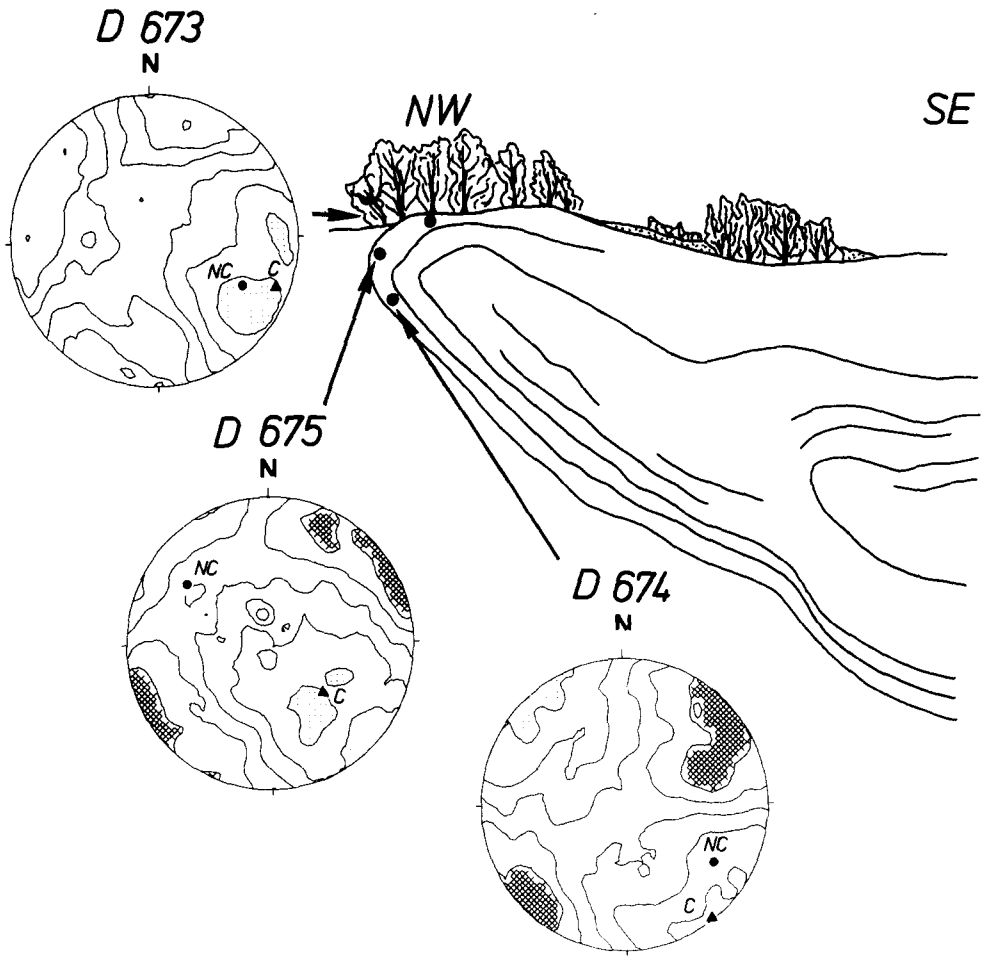

Fig. 12. F_1 fold at La Routia, Lower Cretaceous limestones. The bedding planes are folded by an F_1 fold. The pole figures, upper-hemisphere equal-area projections, are in geographical coordinates. c, *c*-axis maximum; NC, normal to the bedding. The intensity maximum is 1.6 for all three pole figures.

of the Morcles nappe are related to the strain pattern arising during the development of these folds. The deformation histories inferred from the fabric for the Saillon and Petit Pré folds can be integrated with the regional deformation history of the nappe. Fold formation appears to be best related to conditions of predominant simple shear displacement in the root zone of the inverted limb, whereas in the core of the nappe the displacements leading to folding were those predominant in flexural-slip buckle folds. This change in deformational regime is also expressed in the morphology of the folds. The axial plane of the Saillon fold is at a low angle to the basal thrust contact of the nappe, whereas the axial plane of the Petit Pré fold is at a high angle to it. This variation in the dip of the axial planes, as well as the different deformation histories of the two folds, can be explained by a 'locking' of the frontal folds of the nappe during the second phase of deformation. The overall regional strain pattern expected for such a situation is comparable to that of a shear zone termination (Ramsay & Allison 1979). The observed change in dip of the fold axial planes is in agreement with this theoretical model.

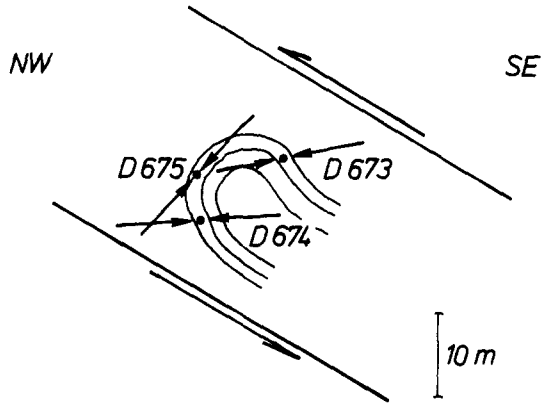

Fig. 14. A model for the development of the F_1 fold at La Routia. The compression directions inferred from the textures are indicated. The fold is represented in a profile section.

The *c*-axis directions around the Neimia second-phase fold indicate that this kink fold is younger than the fabric but that the fabric overprints and is later than the phase-1 cleavage.

Figure 15 represents a summary of the data collected from the folds studied, from which the following inferences can be made.

(1) The normals to the cleavage and the *c*-axis maxima for the three second-phase folds (Saillon, Petit Pré and Neimia) are approximately situated on the same great circle. This suggests that the crystallographic preferred orientation and the second-phase folding were acquired during the same kinematic event. Such a pat-

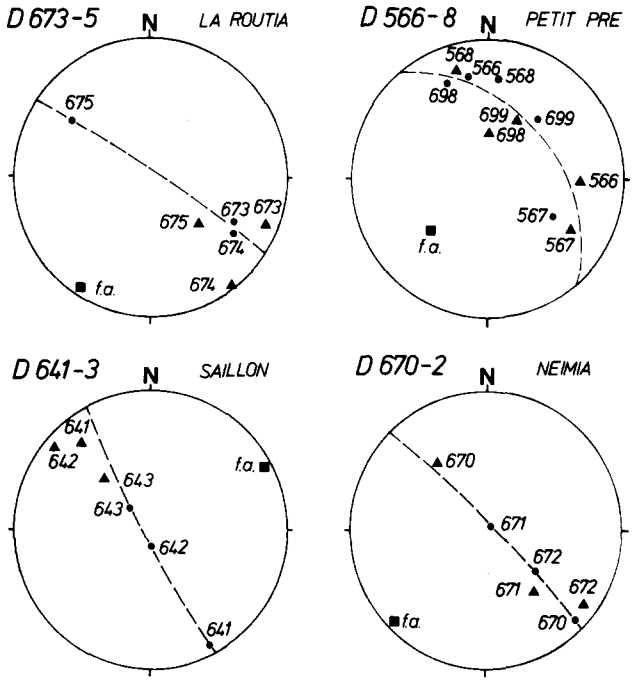

• NORMAL TO THE CLEAVAGE. FOR THE LA ROUTIA FOLD NORMAL TO THE BEDDING.
▲ C-AXIS POINT MAXIMUM

Fig. 15. Synoptic upper-hemisphere equal-area projections of the fabric data obtained for the F_1 fold at La Routia and for the F_2 folds at Saillon, Petit Pré and Neimia. f.a., fold axis.

tern is expected in the Saillon and Petit Pré folds, where fabric and folding are genetically linked. The analysis of the Neimia fold shows that the kinematic events which produced the fabrics and the fold had the same direction.

(2) For the first-phase fold (La Routia) the *c*-axis maxima from different localities in the fold are grouped together to form a point maximum, indicating that the calcite preferred orientation overprints the fold.

(3) The calcite preferred orientation and the grain shape fabric are always parallel, that is, the *a*-girdles are parallel to the grain flattening plane.

(4) The calcite *a*-girdles in the pole figures around the folds generally have positions parallel to those of second-phase cleavage planes. Around the Saillon fold the variable position of the *a*-girdles can be correlated with the cleavage variations in a fold-related fan. Even where a macroscopically visible cleavage fan is absent (Petit Pré) the *a*-great circles appear to be geometrically consistent with a potential fan-shaped orientation of principal *XY* strain planes produced during the folding.

(5) In all the pole figures the *a*-maxima contained in the great circles lie in a region close to the fold axis. This is not consistent with Kern's (1977) experimental results. Kern (1977) deformed Carrara marble under a general triaxial stress at 400°C and found that the *a*-maxima align with the 'unique principal axis of extension'. This suggests that his specimens were deformed by a mechanism different from that of the Helvetic limestones. Additional work needs to be carried out to relate field and experimental fabric data.

Acknowledgements—John Ramsay has critically read the manuscript. Martin Casey has written the rotation program for the pole figures. He and John Ramsay are warmly thanked for their interest in this project, as well as for many helpful discussions. Stefan Schmid is thanked for reviewing this article. Financial support from Schweizerischer Nationalfonds (project no. 2.325-0-81) is gratefully acknowledged.

REFERENCES

Badoux, H. 1971. *Notice Explicative, Feuille* 1305 *Dt. de Morcles*, 1:25'000. Kümmerly & Frey S.A., Bern.

Badoux, H. 1972. *Tectonique de la Nappe de Morcles entre Rhône et Lizerne*. Matériaux pour la Carte Géologique de la Suisse, n.s., Nr. 143.

Casey, M. & Huggenberger, P. 1985. Numerical modelling of finite-amplitude similar folds developing under general deformation histories. *J. Struct. Geol.* **7**, 103–114.

Casey, M., Rutter, E. H., Schmid, S. M., Siddans, A. W. B. & Whalley, J. S. 1978. Texture development in experimentally deformed calcite rocks. *Proc. 5th Int. Conf. Textures of Materials*, Springer, Berlin, 231–240.

Dietrich, D. & Durney, D. W. in press. Change of direction of overthrust shear in the Helvetic nappes of Western Switzerland. *J. Struct. Geol.*

Dietrich, D. & Song, H. 1984. Calcite fabrics in a natural shear environment, the Helvetic nappes of Western Switzerland. *J. Struct. Geol.* **6**, 19–32.

Dietrich, D., Song, H. & Casey, M. 1981. An attempt at a kinematic interpretation of the root zone of the Helvetic nappes, Western Switzerland. *J. Struct. Geol.* **3**, 186–187.

Durney, D. W. 1972. Deformation history of the Western Helvetic nappes, Valais, Switzerland. Unpublished Ph.D. thesis, University of London.

Friedman, M. & Higgs, N. G. 1981. Calcite fabrics in experimental shear zones. In: *Mechanical Behaviour of Crustal Rocks. Geophys. Monogr.* **24**, 11–27.

Kern, H. 1977. Preferred orientation of experimentally deformed limestone marble, quartzite and rock salt at different temperatures and states of stress. *Tectonophysics* **39**, 103–130.

Ramsay, J. G. 1967. *Folding and Fracturing of Rocks*. McGraw-Hill, New York.

Ramsay, J. G. 1980. Shear zone geometry: a review. *J. Struct. Geol.* **2**, 83–99.

Ramsay, J. G. & Allison, I. 1979. Structural analysis of shear zones in an alpinised Hercynian granite. *Schweiz. miner. petrogr. Mitt.* **59**, 251–279.

Ramsay, J. G., Casey, M. & Kligfield, R. 1983. Role of shear in the development of the Helvetic fold-thrust belt of Switzerland. *Geology* **11**, 439–442.

Rutter, E. H. & Rusbridge, M. 1977. The effect of non-coaxial strain paths on the crystallographic preferred orientation development in the experimental deformation of a marble. *Tectonophysics* **39**, 73–86.

Schmid, S. M., Casey, M. & Starkey, J. 1981. The microfabric of calcite tectonites from the Helvetic nappes (Swiss Alps). In: *Thrust and Nappe Tectonics* (edited by McClay, K. & Price, N. J.). *Spec. Publs geol. Soc. Lond.* **9**, 151–158.

Siddans, A. W. B. 1976. Deformed rocks and their textures. *Phil. Trans. R. Soc.* **A283**, 43–54.

Turner, F. J., Griggs, D. T., Clark, R. H. & Dixon, R. H. 1956. Deformation of Yule marble—VII. Development of oriented fabrics at 300–500°. *Bull. geol. Soc. Am.* **67**, 1259–1294.

Wenk, H. R., Venkitsubramanyan, C. S. & Baker, D. 1973. Preferred orientation in experimentally deformed limestone. *Contr. Miner. Petrol.* **38**, 81–114.